University of Queensland, Brisbane, Australia, August 1973, pp.1-8.

FREE VIBRATION OF RECTANGULAR BARS

by

B. AALAMI and H. JAVAHERIAN

(Arya-Mehr University of Technology, Tehran)

SUMMARY. Based on the extended Rayleigh-Ritz energy method an analysis is outlined for free vibrations of orthotropic uniform long prismatic bars. The method, being general, is used in a comprehensive study of the vibrations of rectangular bars having cross-sectional aspect ratios 1 to 6, and covering the range of wavelengths from 1 to 1000 times the cross-sectional width. The results offered provide a complete and accurate documentation of the vibrational behaviour of square bars. A general definition for mode and branch designation is proposed for bars of rectangular cross-section. The solutions are compared with the previous work and the differences pointed out. The effects on frequency, of variations in Poisson's ratio and material properties are discussed.

I INTRODUCTION

(a) General

Exact solutions to the problem of free vibrations and elastic wave propagation in infinite bars have only been possible for the circular cross-section. For other cross-sections, which constitute an extremely important area of study in geophysics (seismology), crystal physics (ultrasonics), electronics (acoustic wave guides) and composite materials, up to date, only limited success is achieved.

Herein, following a brief description of the state of the art, a powerful and general method is outlined for the analysis of elastic wave propagation and vibrations in orthotropic rectangular bars of infinite length (Fig. 1). Based on a thorough and extensive study of the possible configurations obtained for vibrations of solid rectangular bars, a unified mode and branch classification is presented for both the square and rectangular cross sections. The method is subsequently utilised to obtain results for rectangular cross-sections with aspect ratios 1-6. The solutions are compared with those of the previous investigators when available. The tabulated data given provides a new and comprehensive documentation of free vibrations of rectangular bars. The present study concludes with an investigation into the effects of variations in Poisson's ratio and a qualitative description of free vibrations in composites with idealised material properties.

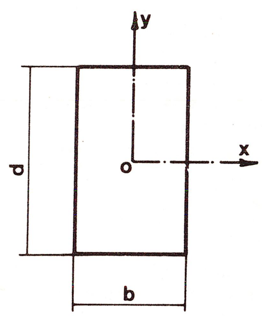

Fig. 1 Coordinate system of the rectangular cross-section.

(b) State of the Art

A review of the available literature, up to 1960, on the methods of evaluation of dispersion relations for non-circular bars is given in (Ref. 1).

For elastic waves in rectangular bars, Mindlin

NOTATION

b = width of cross-section parallel to x-axis;
C_{ij} = elastic moduli;
d = depth of cross-section parallel to y-axis;
G = shear modulus;
$[k]$ = element stiffness matrix;
$[K]$ = assemblage stiffness matrix;
$[m]$ = element mass matrix;
$[M]$ = assemblage mass matrix;
r = radius of gyration about x-x;
$\{r\}$ = nodal values of functions w', u', v';
$\{r_o\}$ = nodal amplitudes of functions w', u', v';
t = time;
T = kinetic energy;
u,v,w = displacements in x,y and z directions respectively;
u', v', w' = displacement functions in terms of x,y and t;
V = potential energy;
x,y,z = Cartesian coordinates;
α = time-dependent coefficients;
ε = strain;
λ = half wavelength;
ν = Poisson's ratio;
ξ = normalised half wavelength $(= \frac{b}{\lambda})$;
ρ = mass density;
σ = stress;
ω = circular frequency;
Ω = normalised frequency $(= \frac{\omega b}{\pi} (\rho/G)^{\frac{1}{2}})$;
Ω_o = normalised frequency referring to a square bar with $\nu = 0.3$;
$(\dot{})$ = differentiation with respect to time.

and Fox (Ref. 2) were among the first to obtain exact solutions for a limited number of aspect ratios and giving a discrete set of points on the dispersion curves. Their method is of limited application and is not general to describe the complete behaviour. Volterra in (Ref. 3) employs the method of internal constraints in conjunction with Hamilton's principle to obtain dispersion curves for the longitudinal vibrations of rectangular bars. The accuracy of the results obtained is not satisfactory even for the first branch.

Using the variational method and series expansion of approximate displacement functions in products of Legendre polynomials to satisfy the field equations and the boundary conditions, Medick (Refs. 4 and 5) treated the problem of longitudinal waves in rectangular bars. His treatment, however, is too complex to apply and no numerical results are presented for finite aspect ratios.

Nigro (Refs. 6, 7 and 8) evaluated the lowest three branches of the longitudinal modes as well as the first flexural and torsional modes using the variational method. The results presented were, as pointed out by Fraser (Ref. 9), not correctly identified.

Employing the method of collocation, Fraser (Ref. 9) enforces the exact solution of the elastic wave equation in cylindrical polar coordinates to satisfy the traction-free boundaries of a rectangular bar at a given set of (collocation) points. The method yields the longitudinal, torsional, flexural and also the depth-stretch and the oblique modes of wave propagation. The latter two are referred to as the first and second screw modes in (Ref. 9) for square bars. The method is reasonably accurate for the first branches and lower aspect ratios (d/b<2).

Hertelendy (Ref. 10) develops variational equations of motion for symmetric deformational configurations and obtains solutions for the longitudinal, depth-stretch and the oblique modes. Having conducted a series of experiments, the adjustment factors introduced in the theory are determined by matching the relating experimental and theoretical values.

In (Ref. 11) the first author presents a formulation for the analysis of elastic waves in orthotropic infinite bars of arbitrary cross-section. The work is an extension of the general Rayleigh-Ritz energy method to incorporate the problem of vibrations and waves in bars of arbitrary cross-section. For the rectangular bars, the cross-section is discretised into mathematical regions called elements. The components of displacement forms representing the waves in the bar are taken as a product of a harmonic function in the propagating direction and an unknown function for each spatial direction. The characterisation of the problem to simple harmonic motion leads to an algebraic eigenvalue problem which is solved by an effective direct-iterative eigensolution technique. The effectiveness of the method and its application to the field of electronics (microsound surface wave guides) are discussed in (Ref. 12). The method extracts a predetermined number of the lowest modes and branches. The accuracy is shown (Ref. 12) to be good and capable of being enhanced if more elements are used to discretise the cross-section.

(c) Mode and Branch Classification

Herein, the term <u>mode</u> refers to the broad classification of the types of waves that propagate in rectangular bars, and <u>branch</u> refers to a particular dispersion curve in the family of dispersion curves belonging to a given mode. For any given wavelength, the branches of each particular mode are numbered in succession from the lowest frequency.

For ease of comparison and cross reference, the vibrational modes and branches are presented in a unified manner for both the square and rectangular bars. The deformation of a bar cross-section under the wave motion is designated by a mode configuration code. The mode designation is necessary for identification. In general, at cutoff frequencies ($\lambda \sim \infty$) the cross-sectional deformations are characterised by simple displacement forms which may be readily categorised into flexural (B), torsional (T), longitudinal (LL), oblique (O) and depth-stretch (LD) modes as described in (Fig. 2).

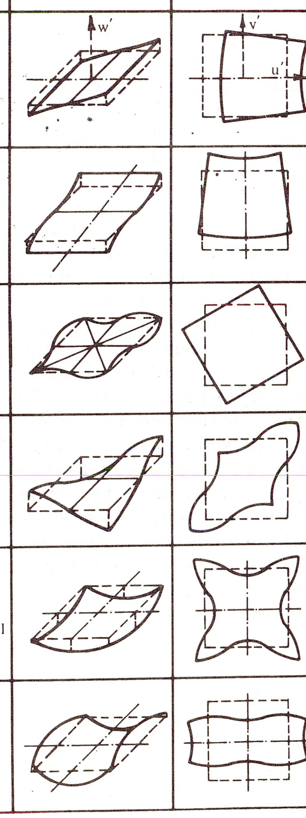

Mode Description	Deformation configuration: w' Displacement	Deformation configuration: u' - v' Displacement	Principal deformation	Description
B_{y1} Flexural			u'	Symmetrical about x-x; anti-symmetrical about y-y
B_{x1} Flexural			v'	Anti-symmetrical about x-x; symmetrical about y-y
T_1 Torsional			u', v'	Anti-symmetrical about x-x and y-y nonzero rotation of diagonals
O_1 Oblique			u', v'	Anti-symmetrical about x-x and y-y zero rotation of diagonals
LL_1 Longitudinal			w'	Symmetrical about x-x and y-y; u and v in phase
LD_1 Depth-stretch			v'	Symmetrical about x-x and y-y; u' and v' 180° out of phase

Fig. 2 Mode designations and displacement configurations for free vibrations of rectangular bars. Broken lines refer to the undeformed cross-section: heavy lines refer to maximum deformation of cross-section.

With reduction in wavelength, the initially smaller displacement components gain in magnitude, such that at wave lengths of the order of cross-sectional sides, the deformations are frequently very complex as illustrated in Fig. 2 for the wavelength ratio $\xi = 1$. The mode designations are based, in each case, on those deformation-characteristics which remain unchanged for all wavelengths and are summerised on the last column of Fig. 2.

II THEORY

For the analysis of steady-state vibrations of elastic isotropic bars (with coordinate axes of Fig. 1), the displacements on a cross-section parallel to x-y plane and at time t, using the finite element approach (Ref. 13), may be taken as follows:

$$w = w'(x,y,t) \sin(\pi z / \lambda)$$
$$u = u'(x,y,t) \cos(\pi z / \lambda) \qquad (1)$$
$$v = v'(x,y,t) \cos(\pi z / \lambda)$$

in which λ is the half wavelength.

The functions w', u' and v' may be resolved into time-dependent generalized coordinates α and position-dependent Cartesian coordinates in the following form:

$$w' = \alpha_1 + \alpha_2 x + \alpha_3 y$$
$$u' = \alpha_4 + \alpha_5 x + \alpha_6 y \qquad (2)$$
$$v' = \alpha_7 + \alpha_8 x + \alpha_9 y$$

From the displacement functions of Eqs. (2) the strain energy of an element of volume dxdydz may be evaluated using Eq. (3)

$$S.E. = \frac{1}{2} \iiint \{\varepsilon\}^T \{\sigma\} dxdydz \qquad (3)$$

where for any given wavelength ratio $\xi (=b/\lambda)$, the strains $\{\varepsilon\}$ at a point are derived by appropriate differentiation of displacement functions. Stresses $\{\sigma\}$ are subsequently expressed in terms of strains using the generalized Hook's law. Similarly for an element of volume dxdydz, with uniform mass density ρ, the kinetic energy is given by:

$$K.E. = \frac{1}{2} \rho \iiint [\dot{w}\ \dot{u}\ \dot{v}] \begin{Bmatrix} \dot{w} \\ \dot{u} \\ \dot{v} \end{Bmatrix} dxdydz \qquad (4)$$

in which the velocities $\dot{w}$, $\dot{u}$ and $\dot{v}$ are derived through differentiation of Eq. (2) with respect to time t.

Now for the application of the extended Ritz energy method or as better known the finite elements, the beam is considered being mathematically subdivided into an assemblage of discrete segments (elements) in form of triangular prisms with their longitudinal axis parallel to the axis of the beam.

The potential energy (V) of each element can be evaluated by integration of Eq. (3) over the volume of the element for the representative length λ and expressed in form of Eq. (5), where $\{r\}$ is the nodal values of functions w', u' and v' from Eq. (2), and $[k]$ is the stiffness matrix of the element.

$$V = \frac{1}{2} \{r\}^T [k] \{r\} \qquad (5)$$

Similarly the representative kinetic energy (T) of an element of length λ may be evaluated by integration of Eq. (4) over the same volume and simplified into Eq. (6):

$$T = \frac{1}{2} \{\dot{r}\}^T [m] \{\dot{r}\} \qquad (6)$$

The Lagrangian L of a representative length λ of the bar is given by the summation over the cross section of the appropriate energies of each element:

$$L = \Sigma(T-V) = \frac{1}{2} \{\dot{r}\}^T [M] \{\dot{r}\} - \frac{1}{2} \{r\}^T [K] \{r\} \qquad (7)$$

where [M] and [K] are respectively the mass and stiffness matrices of the assemblage formed through summation of appropriate terms of elements' stiffness and mass matrices.

Application of Hamilton's principle to the Lagrangian of Eq. (7) gives the equations of motion:

$$[K] \{r\} + [M] \{\ddot{r}\} = 0 \qquad (8)$$

For simple harmonic motion with $\{r_o\}$ being the amplitudes of nodal values of functions w', u' and v' the equations of motion reduce to the following algebraic eigenvalue problem:

$$([K] - \omega^2 [M]) \{r_o\} = 0 \qquad (9)$$

Any of the standard eigenvalue and eigenvector extraction procedures may now be used for the evaluation of frequencies and their corresponding modes and branches from Eq. (9). The present analysis employs an efficient iterative method as outlined in (Ref. 14). The eigenvalue and eigenvector extraction procedure employed evaluates a predetermined number of lowest eigenvalues and their eigenvectors without a priori knowledge of mode configurations or imposition of mode restraints.

III RESULTS

(a) Isotropic Elastic Rectangular Bars

In order to study the variations in natural frequencies with changes in wavelength and also the influences of cross-sectional dimensions, several isotropic rectangular bars of different aspect ratios (1-6) with a Poisson's ratio of 0.3 are analysed. The solutions obtained relate to wavelengths from 1 to 1000 times the cross-sectional width. The range considered adequately covers the longer wavelengths which are of interest in mechanical and structural vibrations and also the short wavelengths of application in electronics and crystal physics.

For the isotropic square bar, the normalised frequencies of the lower modes and branches are listed in Table I. The values given are obtained by modelling the cross-section by 96 triangular elements and specifying an accuracy of 0.0001 for frequencies (eigenvalues). This implies a relative change, in the process of iteration, between the successively improved values of frequencies of less than the specified value.

Table II lists the lower nine branches and modes of a 3 to 1 rectangular bar, which in the so far absence of numerical results for rectangular cross-sections might provide a basis for future comparisons. The cutoff frequencies and the long-wavelength results are summerised in Table III for aspect ratios 1,2,3 and 6.

TABLE I

Homogeneous isotropic solid square bar.
Table of frequencies for various wavelengths.

ξ \ Mode	Frequency ratio $\Omega_o = \frac{\omega b}{\pi}(\rho/G)^{1/2}$, b = side length, ν = 0.3							
	Bx1 By1	Bx2 By2	Bx3 By3	T_1	LL_1	O_1	LD_1	LL_2
0.002	0.0000	1.0062	1.4236	0.0019	0.0032	1.2734	1.4832	2.0696
0.02	0.0006	1.0068	1.4237	0.0186	0.0322	1.2731	1.4589	1.9613
0.2	0.0553	1.0655	1.4348	0.1857	0.3215	1.2536	1.4465	1.8990
0.4	0.1925	1.2104	1.4721	0.3714	0.6367	1.2414	1.4194	1.8856
0.6	0.3694	1.3755	1.5558	0.5574	0.9362	1.2651	1.3987	1.9129
0.8	0.5625	1.4960	1.7230	0.7436	1.2042	1.3260	1.3997	1.9690
1.0	0.7617	1.5913	1.9380	0.9301	1.4210	1.4183	1.4296	2.0480
1.2	0.9627	1.6914	2.2574	1.1171	1.5858	1.5355	1.4893	2.1358
1.4	1.1639	1.8030	2.3860	1.3045	1.7232	1.6712	1.5765	2.2395
1.6	1.3646	1.9269	2.5728	1.4925	1.8554	1.8207	1.6868	2.3549
1.8	1.5645	2.0619	2.7457	1.6810	1.9926	1.9802	1.8159	2.4801
2.0	1.7637	2.2069	2.9036	1.8702	2.1376	2.1473	1.9598	2.6138

TABLE II

Homogeneous isotropic solid rectangular bar (d/b = 3, b parallel to x-axis).
Table of frequencies for various wavelengths.

ξ \ Mode	Frequency ratio $\Omega = \frac{\omega b}{\pi}(\rho/G)^{1/2}$, b = width, ν = 0.3								
	By1	Bx1	By2	Bx2	By3	T_1	LL_1	LD_1	T_2
0.002	0.0000	0.0000	0.3097	0.3342	0.9743	0.0011	0.0032	0.5605	0.6330
0.02	0.0006	0.0017	0.3101	0.3362	0.9743	0.0115	0.0322	0.5597	0.6333
0.2	0.0558	0.1227	0.3533	0.4746	0.9825	0.1207	0.3158	0.5339	0.6595
0.4	0.1953	0.3198	0.4632	0.7057	1.0174	0.2661	0.6822	0.5121	0.7340
0.6	0.3749	0.5192	0.6085	0.9026	1.0864	0.4361	0.9721	0.6268	0.8450
0.8	0.5707	0.7158	0.7726	1.0475	1.1854	0.6213	1.2332	0.7751	0.9807
1.0	0.7724	0.9103	0.9476	1.1910	1.3080	0.8143	1.4292	0.9436	1.1327
1.2	0.9759	1.1036	1.1294	1.3479	1.4482	1.0110	1.5572	1.1227	1.2958
1.4	1.1795	1.2966	1.3156	1.5166	1.6013	1.2096	1.6730	1.3077	1.4667
1.6	1.3827	1.4900	1.5049	1.6938	1.7639	1.4088	1.7976	1.4964	1.6431
1.8	1.5853	1.6839	1.6962	1.8764	1.9336	1.6083	1.9340	1.6878	1.8238
2.0	1.7874	1.8787	1.8890	2.0620	2.1088	1.8079	2.0816	1.8810	2.0077

TABLE III

Homogeneous isotropic solid rectangular bars (width b parallel to x-axis).
Long wavelength and cutoff frequencies of the lower branches.

$\frac{d}{b}$	ξ \ Mode	Frequency ratio $\Omega = \frac{\omega b}{\pi}(\rho/G)^{1/2}$, b = width, ν = 0.3							
		Bx1	By1	T_1	LL_1	Bx_2	By_2	LD_1	T_2
1	0.002	5.8709E-6[a]	5.8709E-6	1.8567E-3	3.2249E-3	1.0062	1.0062	1.4832	1.2734[b]
	0.02	5.8657E-4	5.8657E-4	1.8566E-2	3.2248E-2	1.0068	1.0068	1.4589	1.2731[b]
	0.2	5.5274E-2	5.5274E-2	1.8568E-1	3.2152E-1	1.0655	1.0655	1.4465	1.2536[b]
2	0.002	5.8772E-6	1.1721E-5	1.5025E-3	3.2248E-3	0.5020	0.5681	0.8323	0.9213
	0.02	5.8724E-4	1.1690E-3	1.5026E-2	3.2246E-2	0.5033	0.5683	0.8319	0.9211
	0.2	5.5445E-2	9.6059E-2	1.5196E-1	3.1983E-1	0.6101	0.5961	0.8028	0.9289
3	0.002	5.8936E-6	1.7571E-5	1.1491E-3	3.2248E-3	0.3342	0.3097	0.5605	0.6330
	0.02	5.8898E-4	1.7469E-3	1.1497E-2	3.2244E-2	0.3362	0.3101	0.5597	0.6333
	0.2	5.5802E-2	1.2273E-1	1.2068E-1	3.1583E-1	0.4746	0.3533	0.5338	0.6595
6	0.002	3.5114E-5	5.9410E-6	6.5227E-4	3.2248E-3	0.1669	0.0975	0.2816	0.2367
	0.02	3.4326E-3	5.9395E-4	6.5444E-3	3.2230E-2	0.1707	0.0983	0.2799	0.2372
	0.2	1.5887E-1	5.6748E-2	8.2665E-2	4.8587E-1	0.3527	0.1589	0.2556	0.2829

a 5.8709E-6 ≡ 5.8709 x 10^{-6}

b O_1 branch for square section.

The frequency variations with aspect ratio for the basic modes and the first two flexural branches are illustrated in Fig. 3 for several wavelength ratios. For ease of comparison, the frequencies given are all normalised with respect to the frequencies of the square bar (Ω_o) for the same

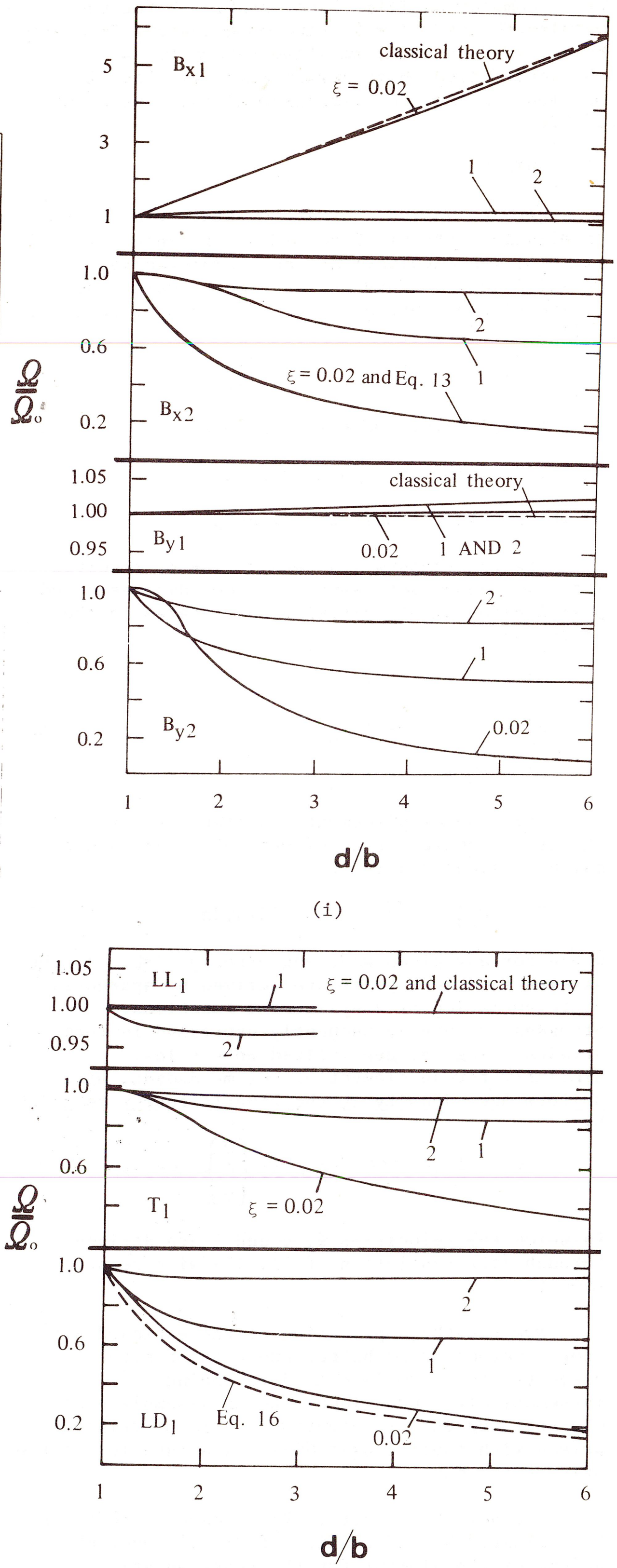

Fig. 3 Variation of frequencies of rectangular bars with aspect-ratio d/b, (Ω_o = the relating frequency of the square bar as given in Table I). Note the change in frequency scale.

wavelength ratios (values of Table I). For the first flexural branch B_{x1}, the frequency equation from the classical theory (Ref. 15) is given by

$$\Omega = 0.233\ (d/b)\ \xi^2 \tag{10}$$

from which the normalised variation with aspect ratio is

$$(\Omega / \Omega_o) = d/b \tag{11}$$

which is an accurate expression of the long wavelength behaviour (ξ = 0.02 as is illustrated in the uppermost portion of Fig. 3-i). For wavelength ratios of the same order of magnitude as the cross-sectional width, the inadequacy of the classical theory is clearly shown in the figure. This shortcoming has long been recognised (Ref. 16) and is attributed to the shearing deformations and the rotatory inertia not accounted for in the classical theory.

For the second flexural branch (B_{x2}), solutions are available for the cutoff frequency, which closely express the long wavelength vibrational behaviour. From (Ref. 17) the cutoff frequency is given by:

$$\omega = \frac{\pi}{r}\ (G/12\,\rho)^{\frac{1}{2}} \tag{12}$$

which in terms of the variables of Fig. 3 reduces to the inverse of the aspect ratio:

$$(\Omega / \Omega_o) = b/d \tag{13}$$

On the scale of Fig. 3-i, the curve of this equation is indistinguishable from the results of the present analysis for wavelength ratio 0.02. Little work is done to accurately express the vibrational behaviour of higher flexural branches at smaller wavelength ratios. A survey of the available work together with new proposals for the improvement of Timoshenko's beam theory and its extension to higher branches is given in (Ref. 18).

For the first flexural branch about y-y (B_{y1}), due to the width being kept constant, the simple theory gives a straight line for all aspect ratios:

$$(\Omega / \Omega_o) = 1 \tag{14}$$

The slight deviations from the straight line in the relating curves of Fig. 3-i may be attributed to the effects of Poisson's ratio not accounted for in the classical theory.

For the first branch of longitudinal vibrations (LL_1), from simple theory, the frequency and aspect ratios are related by Eq. 14 which coincides with its corresponding curve from the present analysis for the long wavelength (ξ=0.02, uppermost portion of Fig. 3-ii). For shorter wavelengths, LL_1 curves are not continued, as for aspect ratios above 3 the LL_1 frequencies fall above the first 12 branches extracted by the iteration procedure.

The behaviour of the first depth-stretch (LD_1) mode may be related to the first symmetric thickness-stretch of an infinite plate on account of their analogous configuration deformations. From (Ref. 19) the thickness-stretch cutoff frequency is given by:

$$\frac{\omega d}{\pi}\ (\rho /G)^{\frac{1}{2}} = [2(1-\nu)/(1-2\nu)]^{\frac{1}{2}} \tag{15}$$

On conversion to the normalised frequency of Fig.4, Eq. (15) simplifies to:

$$(\Omega / \Omega_o) = b/d \tag{16}$$

which as shown at the bottom portion of Fig. 3-ii is a good representation of the long wavelength (ξ = 0.02) behaviour of the rectangular bars' depth-stretch mode. It should be noted that one basic difference between the two problems is the traction-free sides of the rectangular cross-section as compared to the plane-strain idealisation of the infinite plate.

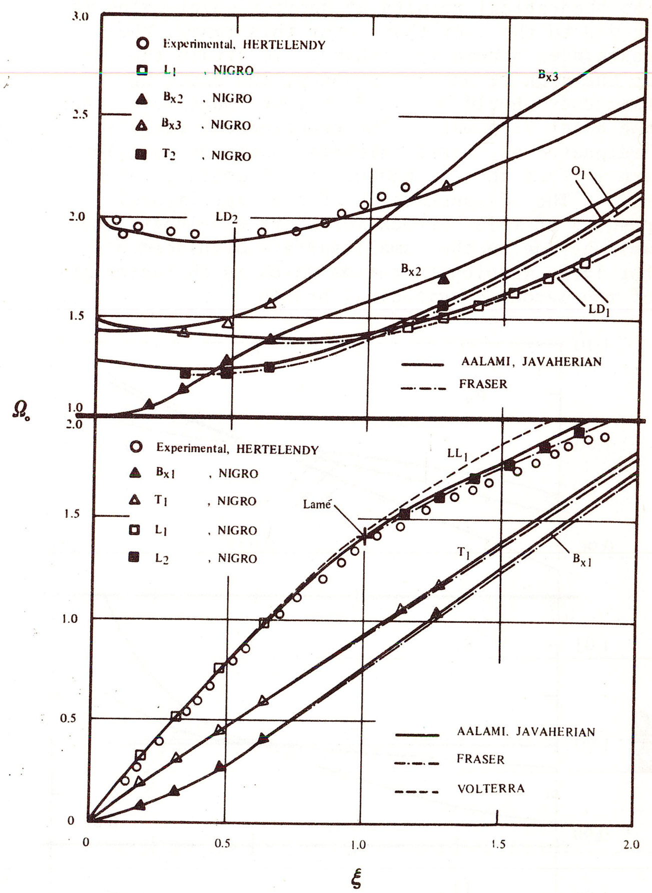

Fig. 4 Homogeneous isotropic solid square bar. Frequency spectrum for real values of ξ from the present analysis and works of other investigators.

Figure 4 gives a comparison between the results of the previous investigations and the present solutions for an isotropic square bar with ν = 0.3. Solutions given by Nigro (Refs. 6,7 and 8), when reinterpreted as suggested by Fraser, agree reasonably well with the present results, specially for the lower branches and smaller wavelength ratios. For example, Nigro's L_1 for ξ = 1 as shown in the upper portion of Fig. 4 is in fact mode LD_1 of the square bar. The solutions given by Fraser (Ref. 9) agree well with the relating branches of the present work, but are consistently lower than the latter. A reliable criterion for the relative degrees of accuracy of the various methods is the accuracy with which each can predict the exact Lamé waves. The value obtained from the method presented herein is 1.4210 for the lowest longitudinal mode as compared with the exact value of $(2)^{\frac{1}{2}}$. Volterra's solutions (Ref. 3) are less accurate compared to the other solutions considered herein. Figure 4 includes only the set of Volterra's results with the closest agreement. Hertelendy's experimental results for the first longitudinal branch fall just below the results of the present work, yet with a fairly good agreement. The different values of Poisson's ratio between the two results, the inherent higher values of eigenvalues given by the variational method, and the structural damping of the experimental bar may be counted as contributory sources of discrepancy between the experimental and the theoretical solutions. The increased differences between the experimental and the theoretical results at shorter wavelengths may be due to the fact that, over this range, the resonances become very sharp. To attain the system at the high resonant frequency, the exciting frequency should be fixed at lower magnitudes than the exact frequency. The experimental results designated as first thickness-shear by Hertelendy are in fact the second branch of depth-stretch mode. The disappearance of the experimental results of this branch for short wavelengths may well be due to the small surface displacements for large wavelength ratios which is characteristic of the second longitudinal branch.

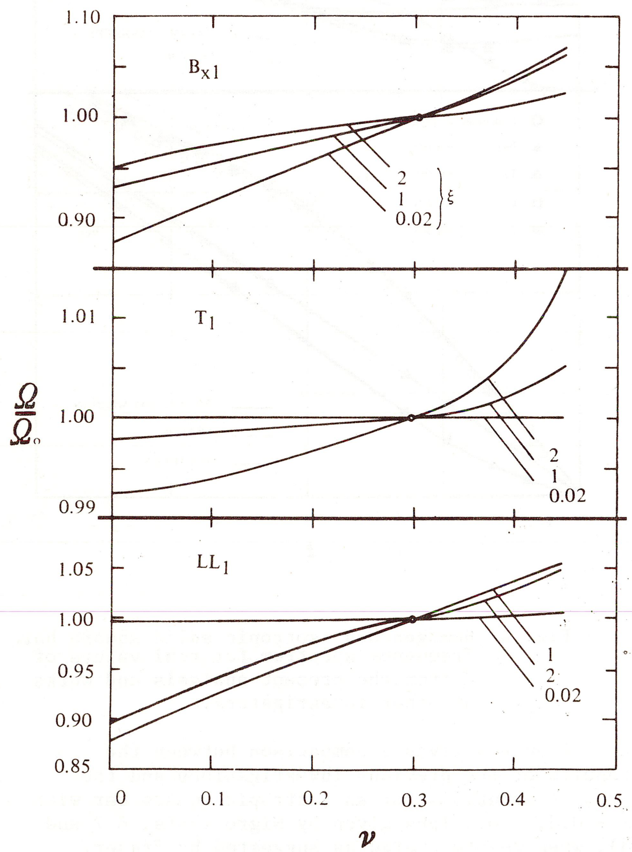

Fig. 5 Variation of frequencies of a square isotropic bar with Poisson's ratio, (Ω_0= the relating frequency of the square bar as listed in Table I with ν=0.3).

(b) Variations in Poisson's Ratio

The influences of variations in Poisson's ratio on the frequencies of the first flexural (B_{x1}), torsional (T_1) and longitudinal (LL_1) are illustrated in Fig. 5. For each of the aforementioned modes the variations of the normalised frequencies for three wavelength ratios are shown for Poisson's ratios 0 to 0.45. At each point the frequencies are normalised with respect to the relating frequency and wavelength ratio of the square bar with a Poisson's ratio of 0.3. The results indicate that generally a decrease in Poisson's ratio is accompanied by a decrease in the natural frequency, and that the frequencies of the first torsional mode are not so sensitive to the variations in Poisson's ratio as the other modes.

(c) Orthotropic Bars

Materials made up of long stiff fibers or layers deliberately orientated in a single direction and embedded in a softer matrix, serve as the basic building blocks of many laminated composites and are gaining increased application due to their superior material properties. The dynamic reponses of unidirectional filamentary as well as laminated composites are of special interest because of their potentially important properties as pulse-attenuation mechanisms (Ref. 20).

One approximate method of treating the composites is to smear out the stiffness of the reinforcing fibers uniformly over the cross-section and model the component as a homogeneous orthotropic material. While this may not reveal the detailed interaction features of the composite constituents, it is believed, the results serve as a good qualitative expression of the influences of various fiber-matrix compositions on frequencies. In order to investigate the effects of fiber-matrix ratios on the dispersion characteristics, five homogeneous elastic orthotropic materials with normalised elastic moduli as listed in Table IV are considered.

TABLE IV

PROPERTIES OF THE ORTHOTROPIC MATERIALS CONSIDERED

Material	No.	Normalised elastic moduli[a]								
		C_{11}	C_{12}	C_{13}	C_{22}	C_{23}	C_{33}	C_{44}	C_{55}	C_{66}
Isotropic	1	3.5	1.5	1.5	3.5	1.5	3.5	1	1	1
Unidirectional, weak[b]	2	0.35	0.15	0.15	0.35	0.15	3.5	0.1	1	1
Undirectional, very weak	3	0.035	0.015	0.015	0.035	0.015	3.5	0.01	1	1
Layered, weak[c]	4	3.5	0.15	1.5	0.35	0.15	3.5	1	1	1
Layered, very weak	5	3.5	0.015	1.5	0.035	0.015	3.5	1	1	1

a Isotropic material (ν = 0.3) and materials 4 and 5 normalised with respect to C_{44} = G, materials 2 and 3 normalised with respect to C_{55}.

b Unidirectionally reinforced in direction of propagation (3-3 axis), weak matrix.

c Layered parallel to direction of propagation, weak matrix.

Material 1 is isotropic with Poisson's ratio of 0.3 and is used as reference. Materials 2 and 3 represent smeared unidirectional filamentary composites having weak and very weak matrices. Materials 4 and 5 refer to composites with stiff layers parallel to x-axis (Fig. 1), and with weak and very weak matrices, respectively. The normalised frequencies obtained for wavelength ratios 0 to 2 are shown in Fig. 6 for the lower modes. It should be emphasised here that the frequencies are each normalised with respect to its relating C_{44} or C_{55} as noted in Table IV.

In Fig. 6 the results of the unidirectional and layered materials each bear the correct relationship to its own weak and very weak cases, but for a quantitative comparison of the two types the relating moduli must be implemented first.

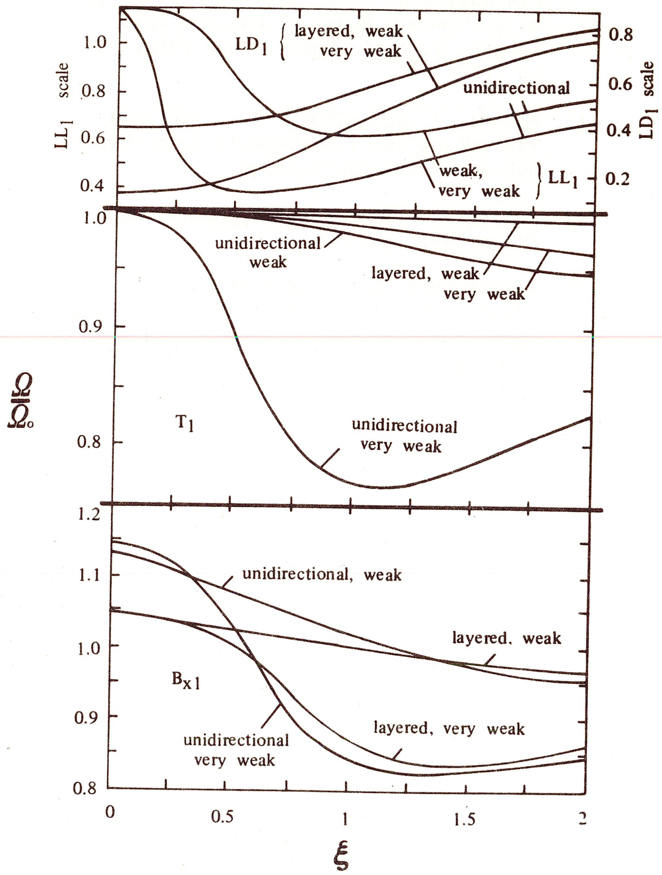

Fig. 6 Idealised unidirectional filamentary and layered composite materials. Frequency spectrum for real values of ξ for flexural, torsional, depth-stretch and longitudinal modes. Material properties as given in Table IV.

IV CONCLUSIONS

A method presented for the effective analysis of free vibrations of rectangular bars is used to evaluate frequency spectrums for elastic isotropic rods having aspect ratios 1-6. The results of the present analysis are related and compared with the previous theoretical and experimental works. The agreement between the present solutions and the existing ones are found to be generally good. A set of new data is offered for rectangular cross-sections, for which no accurate and comprehensive documentation appears to have been published before.

The frequency variation with aspect ratio is investigated and compared with the classical theory of vibrations of beams. It is concluded that the classical theories satisfactorily express the vibrational behaviour only over the long wave-length range. For medium and short wavelengths, there appears to be no approximate theories available for the determination of torsional, longitudinal and depth-stretch modes.

A study in the effects of Poisson's ratio revealed that in general a decrease in Poisson's ratio is accompanied by a decrease in frequency.

The unidirectional filamentary and layered composites are idealised as orthotropic homogeneous materials. The solutions offered for their dynamic behaviour provide a useful basis for the understanding of their vibration characteristics.

V ACKNOWLEDGEMENT

The computations presented herein were carried out in the Arya-Mehr University AMUT-CDC Computer Centre. The authors wish to record their appreciation for the assistance and the prompt services received. The authors are also grateful to Miss C. Grigorian for her extra care and patience in typing this manuscript.

VI REFERENCES

1. GREEN, W.A. - Progress in Solid Mechanics. North-Holland Publ. Co., Amsterdam., Vol. 1 1960, pp. 225-261.

2. MINDLIN, R.D. and FOX, E.A. - Vibrations and Waves in Elastic Bars of Rectangular Cross Section. J.Appl. Mech., Vol. 27, 1960, pp. 152-158.

3. VOLTERRA, E. - Second Approximation of Method of Internal Constraints and its Applications. Int. J. Mech. Sci., Vol. 3, 1961, pp. 47-67.

4. MEDICK, M.A. - One-dimensional Theories of Wave Propagation and Vibrations in Elastic Bars of Rectangular Cross Section. J. Appl. Mech., Vol. 33, 1966, pp. 489-495.

5. MEDICK, M.A. - On Dispersion of Longitudinal Waves in Rectangular Bars. J. Appl. Mech., Vol. 34, 1967, pp. 714-717.

6. NIGRO, N.J. - Wave Propagation in Anisotropic Bars of Rectangular Cross-Section. Part I-Longitudinal Wave Propagation. J. Acoust. Soc. Am., Vol. 43. No. 5, 1968, pp. 958-965.

7. NIGRO, N.J. - Steady - State Wave Propagation in Infinite Bars of Noncircular Cross Section. J. Acoust. Soc. Am., Vol. 40, No. 6, 1966, pp. 1501-1508.

8. NIGRO, N.J. and ANDREWS, R. - Wave Propagation in Anisotropic Bars of Rectangular Cross Section. II-Flexural Wave Propagation. J. Acoust. Soc. Am., Vol. 46, No. 3, Part 2, 1969, pp. 439-642.

9. FRASER, W.B. - Stress Wave Propagation in Rectangular Bars. Int. J. Solids and Structures, Vol. 5, 1969, pp. 379-397.

10. HERTELENDY, P. - An Approximate Theory Governing Symmetric Motions of Elastic Rods of Rectangular or Square Cross Section. J. Appl. Mech., Vol.35, 1968, pp. 333-341.

11. AALAMI, B., - Waves in Prismatic Guides of Arbitrary Cross Section, J. of Appl. Mech., Pending Publication.

12. AALAMI, B. - Analysis and Behaviour of Microsound Surface Wave Guides. Transactions on Sonics and Ultrasonics, IEEE, Vol. SU-20, No. 3, July 1973.

13. ZIENKIEWICZ, O.C. - The Finite Element Method in Engineering Science, McGraw-Hill, London. 1971, 522pp.

14. DONG, S.B., WOLF, J.A. and PETERSON, F.E.- On a Direct-Iterative Eigensolution Technique, Int. J. Numerical Methods in Engineering, Vol. 4, No. 2, 1972, pp 155-161.

15. TIMOSHENKO, S. - Vibration Problems in Engineering, Van Nostrand Co., Inc. New York, N.Y., 1967. 468 pp. .

16. TIMOSHENKO, S. - On the Transverse Vibrations of Bars of Uniform Cross-Section, Philosophical Magazine, Vol. 43, 1922, pp. 125-131.

17. GOODMAN, L.E. and SUTHERLAND, J.G. Discussion of Paper-Natural Frequencies of Continuous Beams of Uniform Span Length, J. Appl. Mech., June 1951, pp. 217-218.

18. AALAMI, B. and ATZORI, B. - Flexural Vibrations and Timoshenko's Beam Theory, Submitted for Publication.

19. KRAUS, H. - Thin Elastic Shells, John Wiley,1967, p. 358.

20. BARTHOLOMEN, R.A. and TORVIK, P.J. - Elastic Wave Propagation in Filamentary Composite Materials, Int. J. of Solids and Structures, Vol. 8, 1972, pp. 1389-1405.

SUPPLEMENT

TO

FREE VIBRATIONS OF RECTANGULAR BARS.

B. Aalami, DIC, PhD, MICE, MRINA, CEng.
Associate Professor of Structural Mechanics

H. Javaherian, BSc
Assistant Lecturer of Mechanical Engineering

Arya-Mehr University of Technology
Tehran P.O.Box 3406, IRAN

Proceedings of the Fourth Australasian Conference on the Mechanics of Structures and Materials, Brisbance, Australia, Aug., 1973.

Mode configurations and frequencies of free vibrations of an isotropic square bar with Poisson's ratio of 0.1.

W DISPL. U-V DISPL.

$\xi = 0.2$

MODE NO. 1

FRE.= 5.10726551E-02

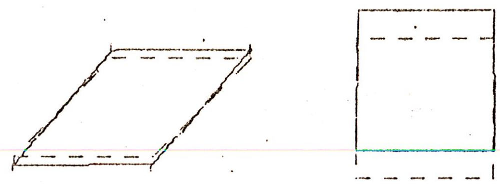

MODE NO. 2

FRE.= 5.10726551E-02

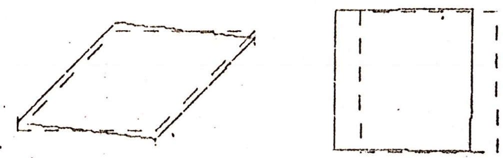

MODE NO. 3

FRE.= 1.90410344E-01

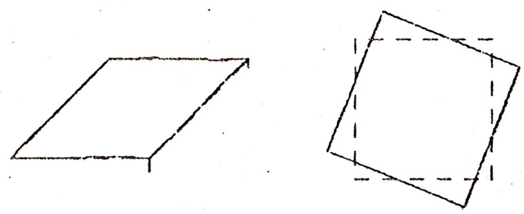

MODE NO. 4

FRE.= 2.96543399E-01

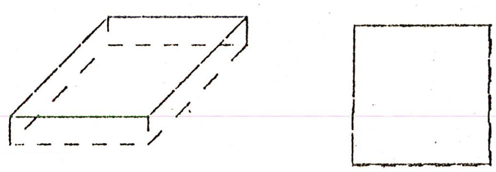

MODE NO. 5

FRE.= 1.07953670E+00

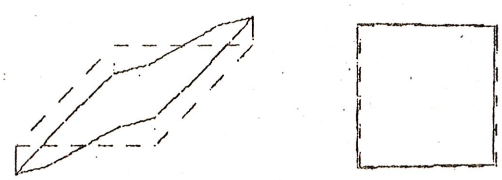

MODE NO. 6

FRE.= 1.07953672E+00

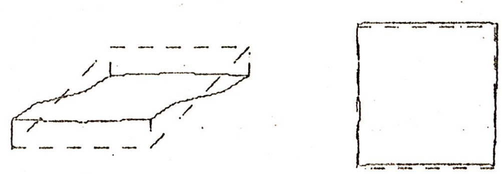

$\xi = 0.2$

MODE NO. 7

FRE.= 1.28941986E+00

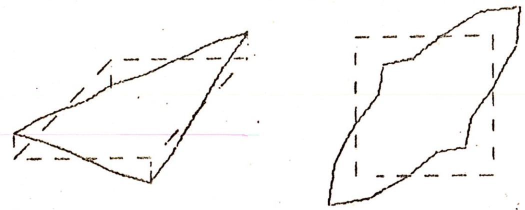

MODE NO. 8

FRE.= 1.39653076E+00

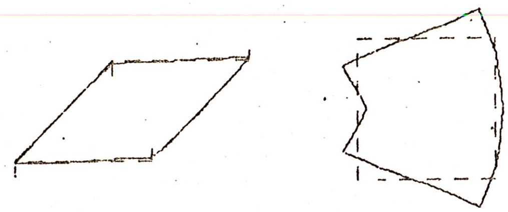

MODE NO. 9

FRE.= 1.39655268E+00

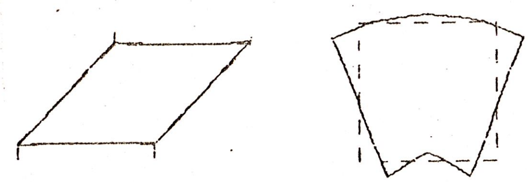

MODE NO.10

FRE.= 1.45163768E+00

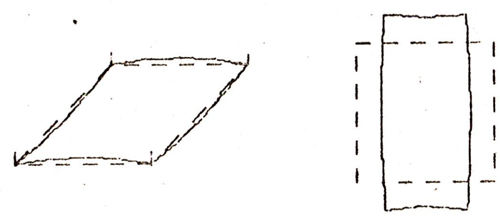

MODE NO.11

FRE.= 1.54062933E+00

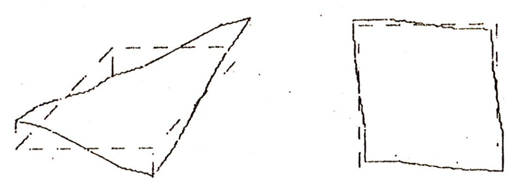

MODE NO.12

FRE.= 1.59036776E+00

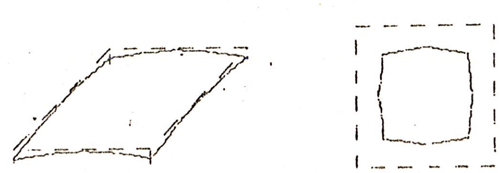

W DISPL. U-V DISPL.

$\xi = 1.0$

MODE NO. 1

FRE.= 7.35094826E-01

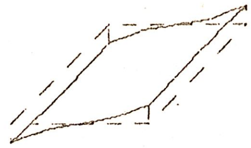

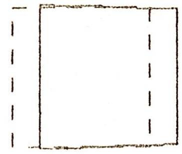

MODE NO. 2

FRE.= 7.35094827E-01

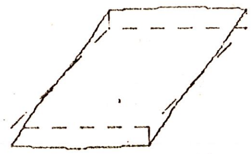

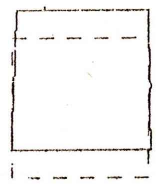

MODE NO. 3

FRE.= 9.54314381E-01

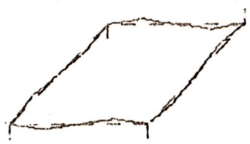

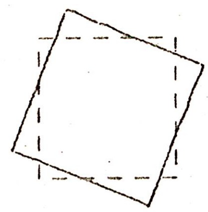

MODE NO. 4

FRE.= 1.41222503E+00

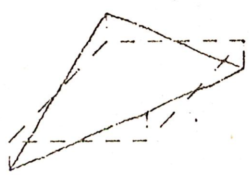

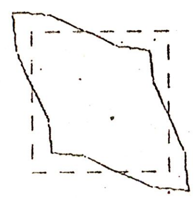

MODE NO. 5

FRE.= 1.43003118E+00

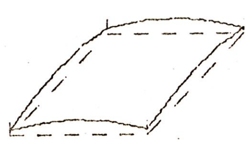

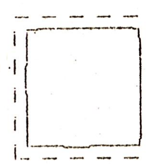

MODE NO. 6

FRE.= 1.45892519E+00

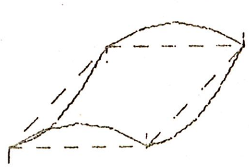

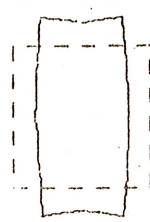

ξ= 1.0

MODE NO. 7

FRE.= 1.62310301E+00

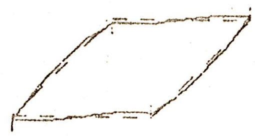

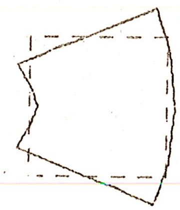

MODE NO. 8

FRE.= 1.62312447E+00

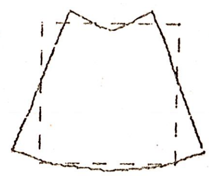

MODE NO. 9

FRE.= 1.63629157E+00

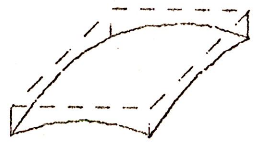

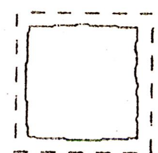

MODE NO.10

FRE.= 1.87451195E+00

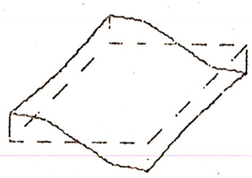

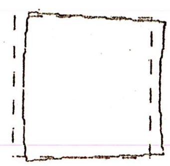

MODE NO.11

FRE.= 1.87451856E+00

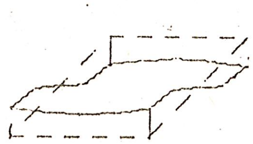

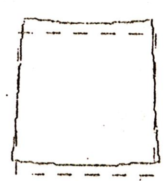

MODE NO.12

FRE.= 2.20205063E+00

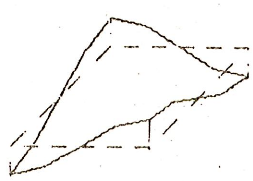

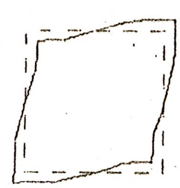

W DISPL. U-V DISPL.

$\xi = 2.0$

MODE NO. 1

FRE.= 1.74345345E+00

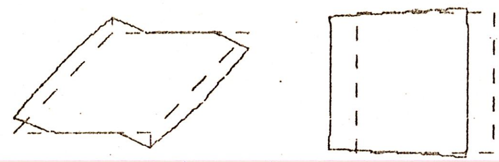

MODE NO. 2

FRE.= 1.74345349E+00

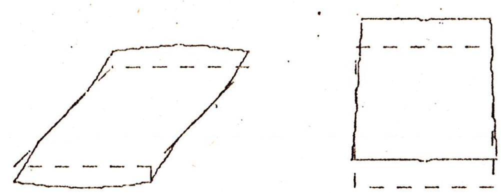

MODE NO. 3

FRE.= 1.92035829E+00

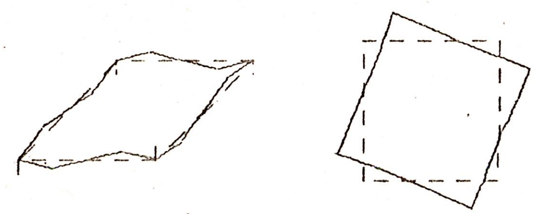

MODE NO. 4

FRE.= 1.98649504E+00

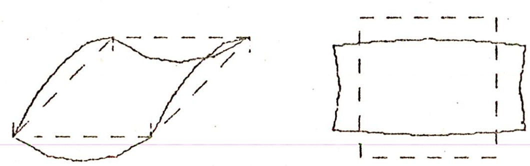

MODE NO. 5

FRE.= 2.05616460E+00

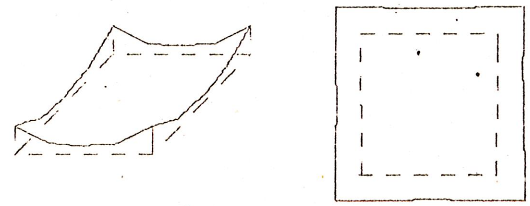

MODE NO. 6

FRE.= 2.11960667E+00

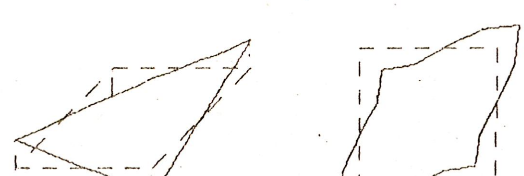

$\xi = 2.0$

MODE NO. 7

FRE.= 2.25221148E+00

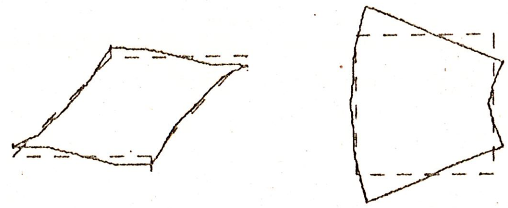

MODE NO. 8

FRE.= 2.25226714E+00

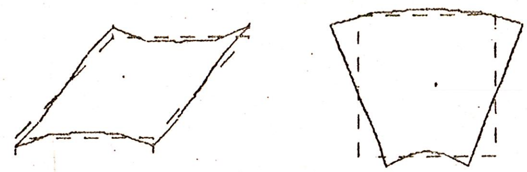

MODE NO. 9

FRE.= 2.80919879E+00

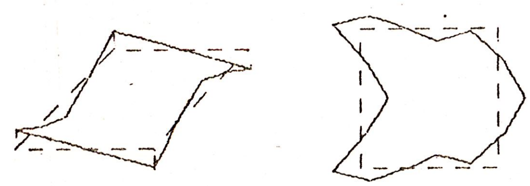

MODE NO.10

FRE.= 2.86239587E+00

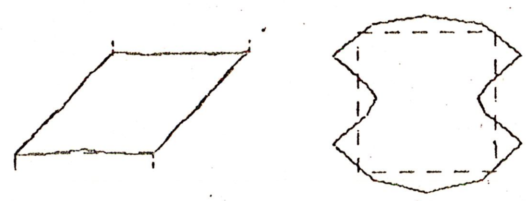

MODE NO.11

FRE.= 3.00096881E+00

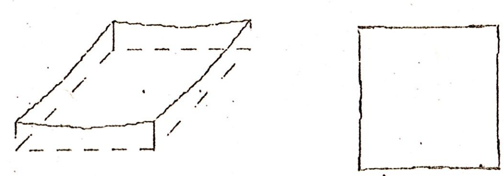

MODE NO.12

FRE.= 3.01294332E+00